Apparent Two Energy Gaps in Pure Niobium[†]

F. Carsey, R. Kagiwada,[*] and M. Levy[‡]

Department of Physics, University of California, Los Angelas, California 90024

and

K. Maki

Physics Department, Tohoku University, Sendai, Japan

(Received 6 March 1970)

It is found experimentally that two energy gaps are obtained for some pure superconductors when ultrasonic attenuation data are analyzed in terms of a simple BCS expression $\alpha_s/\alpha_n = 2/(e^{\Delta(T)/T} + 1)$ for the ratio of the attenuation coefficient in the normal and in the superconducting state. The energy gap $\Delta(T)$ determined in the vicinity of the transition temperature T_c is usually larger than that expected from the low-temperature value $\Delta(0)$. The above BCS expression is valid either in the limit $ql \gg 1$ or if the electronic mean free path l is mainly determined by impurity scattering, where q is the sound wave vector. However, when $ql \ll 1$ and when the sample becomes pure enough that electron-phonon scattering dominates the electron lifetime, we expect an important deviation from the above relation. A theory is proposed which takes into account the effect of the electron-phonon scattering explicitly. This theory predicts that the ratio of the energy gap deduced from high-temperature data (i.e., $T \cong T_c$ the transition temperature) to the one deduced from low-temperature data is a universal function of $x = l_0 B T^3$, where l_0 is the electron mean free path due to impurity scattering while $(BT^3)^{-1}$ is that due to electron-phonon scattering; the electron mean free path in the normal state is given by $l_n^{-1} = l_0^{-1} + BT^3$. In order to have a T^3 dependence, it is assumed that niobium has two distinct electron bands with different effective masses. Making use of the ultrasonic attenuation data in the normal state, we can determine l_n and therefore the parameter x. The ratio of the two energy gaps is then calculated by substituting this value of x into a universal function $f(x)$ which is theoretically derived. It is found that the predicted ratio accounts for roughly one-half of the observed deviation from unity of this ratio. Alternatively, if we use the ratio of the energy gaps to determine x, we find that x (i.e., the electron-phonon scattering contribution) in the superconducting state is three times as large as that determined in the normal state. We are unable to account for these discrepancies at present, although we feel that the observed ratio of the two energy gaps is mostly due to the electron-phonon interaction. However, we cannot completely disregard other possible explanations like the anisotropy of the energy gap or the strong-coupling effect. A numerical estimate of B making use of the known parameters like the electron-phonon coupling constant λ_0 and the Debye frequency ω_D of niobium, on the other hand, yields $B \cong 1.2/K_0^3$ cm in semiquantitative agreement with the value determined experimentally.

I. INTRODUCTION

The BCS theory[1,2] predicts the ultrasonic attenuation coefficient in a superconductor having energy gap $\Delta(T)$ at temperature T:

$$\frac{\alpha_s}{\alpha_n} = \frac{2}{e^{\Delta(T)/T} + 1} . \tag{1}$$

This expression is derived on the assumption either that the electron mean free path is mostly due to the impurity scattering or that the sound wavelength is much shorter than the electronic mean free path.[3-6] If the energy gap is taken to have a BCS temperature dependence, the above ratio is used to determine a unique zero-temperature gap $\Delta(0)$.

If this procedure is used, however, for some pure metals, it is found that the gap parameter $\Delta(0)$ is not constant but has two well-defined limits[7-11]; for data taken close to the superconducting transi-

tion temperature T_c, $\Delta(0)$ appears larger than that determined from data close to $T = 0\,°K$. We will consider the latter value to be more fundamental and will call it the "BCS gap" or $\Delta_{BCS}(0)$. The higher-temperature one we will call the apparent energy gap $\Delta_{ap}(0)$. The purpose of this work is to establish a relationship between these two quantities.

II. THEORETICAL CONSIDERATIONS

As already mentioned in Sec. I, the BCS expression is not valid in a pure specimen when the electronic mean free path is limited mostly by electron-phonon scattering rather than by impurity scattering, since in this case the electronic mean free path depends strongly on both the quasiparticle energy gap and the temperature. In order to treat the electron-phonon interaction explicitly, we consider Fröhlich's model Hamiltonian for a superconductor.

Furthermore, we limit ourselves to the case $ql \ll 1$, where l is the electronic mean free path and q is the sound wave vector for simplicity.

The effect of the electron-phonon scattering on the ultrasonic attenuation coefficient is determined, if we know both the self-energy correction and the vertex correction associated with the sound wave vertex. We will consider briefly these corrections in the following.

A. Self-Energy Correction

The self-energy correction of the electron Green's function due to the electron-phonon scattering in a superconductor has been discussed already by Eliashberg.[12] Here we are only interested in the imaginary part of the correction which gives rise to an electron lifetime.

The renormalized Green's function then is written as

$$G(\omega, \vec{p}) = \frac{\tilde{\omega} + \xi_{\vec{p}}}{\Omega(\omega, \vec{p})} , \qquad F(\omega, \vec{p}) = \frac{\tilde{\Delta}}{\Omega(\omega, \vec{p})} , \qquad (2)$$

where

$$\Omega(\omega, \vec{p}) = \tilde{\omega}^2 - \xi_{\vec{p}}^2 - \tilde{\Delta}^2 , \qquad \xi_{\vec{p}} = p^2/2m - \mu , \qquad (3)$$

$$\tilde{\omega} = \omega + \frac{\pi i \lambda_0}{\omega_0^2} \int_\Delta^\infty d\epsilon' \frac{\epsilon'}{(\epsilon'^2 - \Delta^2)^{1/2}} $$

$$\times \left(\frac{2(\epsilon'^2 + \omega^2)}{e^{\epsilon'/T} + 1} + \frac{2\epsilon'^2 d\epsilon'}{e^{\epsilon'/T} - 1} \right) , \qquad (4)$$

and

$$\tilde{\Delta} \cong \Delta + \frac{\pi i \lambda_0}{\omega_0^2} \int_\Delta^\infty d\epsilon' \frac{\Delta}{(\epsilon'^2 - \Delta^2)^{1/2}} \left(\frac{4\omega\epsilon'}{e^{\epsilon'/T} + 1} \right) . \qquad (5)$$

Here we assumed $\omega \geq 0$, $\lambda_0 = |g| N(0)$, the electron-phonon coupling constant and $\omega_0 = 2s|\vec{p}_0|$ with s the sound velocity and $\vec{p}_0$ the Fermi momentum. In deriving Eqs. (4) and (5) we neglect small correction terms. For these calculations and analysis the Frölich model of electron-phonon interaction has been used. In the vicinity of the transition temperature where $\Delta \ll T$, Eqs. (4) and (5) are further simplified as

$$\tilde{\omega} = \omega + \frac{\pi \lambda_0 i}{\omega_0^2} [7\zeta(3)T^2 + 2\omega^2(-\ln 2)]T \qquad (6)$$

and

$$\tilde{\Delta} = \Delta + \frac{\pi \lambda_0 i}{\omega_0^2} [2\Delta\omega(-\ln 2)]T , \qquad (7)$$

respectively, where $\zeta(3)$ (= 1.202) is Riemann's ζ function. From these expressions the lifetime of the quasiparticle is given as

$$\frac{1}{\tau_{ph}(\omega)} = 2 \operatorname{Im}(\tilde{\omega}^2 - \tilde{\Delta}^2)^{1/2} = \frac{\omega}{(\omega^2 - \Delta^2)^{1/2}} a_1 \theta(\omega - \Delta) \qquad (8)$$

and

$$a_1 = \frac{2\pi\lambda_0}{\omega_0^2} [7\zeta(3)T^2 + 2\omega^2(-\ln 2)]T$$

$$= Bv_0 T^3 , \qquad (9)$$

v_0 being the Fermi velocity. The second term in Eq. (7) is less important than the first term in the whole energy range of interest (i.e., $\omega \lesssim T$), and we neglect this term in the last expression. So far we have neglected the scattering due to impurities. This effect simply adds a constant term to Eq. (8).[13] Thus, the total electron lifetime τ is given as

$$\frac{1}{\tau} = \frac{1}{\tau_{imp}} + \frac{1}{\tau_{ph}(\omega)} . \qquad (10)$$

It is important to note that the lifetime due to impurity scattering is constant (i.e., independent of quasiparticle energy) and the same as the one in the normal state, while that due to the electron-phonon interaction depends strongly on the quasiparticle energy.

A similar energy-dependent lifetime has been introduced previously in a heuristic way by Kadanoff and Martin[14] in their treatment of the thermal conductivity of relatively pure superconductors. In the calculation of the thermal conductivity, we neglect completely the vertex correction due to the electron-phonon scattering, since the vertex correction represents the elastic part of the electron-phonon scattering, which is always extremely small. The relevant lifetime for the thermal conductivity is given by

$$\frac{1}{\tau_{th}} = \frac{1}{\tau_{tr}} + \frac{1}{\tau_{ph}} , \qquad (11)$$

that is, the impurity contribution has to be replaced by the transport lifetime τ_{tr}[13]:

$$\frac{1}{\tau_{tr}} = n \pi N(0) \int |u(\theta)|^2 (1 - \cos\theta) d\Omega , \qquad (12)$$

while

$$\frac{1}{\tau_{Im}} = n \pi N(0) \int |u(\theta)|^2 d\Omega . \qquad (13)$$

Here n is the impurity concentration and $\bar{u}(\theta)$ is the Fourier transform of the impurity potential. The difference between τ_{tr} and τ_{Im} lies in the fact that τ_{Im} represents the electron lifetime due to impurity scattering, while τ_{tr} represents the lifetime of a current carried by the electron.

In the case of the ultrasonic attenuation, however, the vertex correction is of fundamental importance, and we will treat this correction briefly in the following.

B. Vertex Correction

The vertex correction is expressed in terms of ladder-type diagrams; the summation of this series

of diagrams leads to an integral equation. The solution of this integral equation for a superconductor is a rather difficult task. We will not go into details here but within a first-order approximation in λ_0 we have an integral equation for the vertex function:

$$\Lambda(\tau\omega_n,\ i\omega_{n+\nu}) = 1 + \frac{\lambda_0 T}{\omega_0^2} \sum_\mu \int_0^{\omega_0} y\,dy\ P_2\left(1 - \frac{2y^2}{\omega_0^2}\right)$$

$$\times \frac{1}{\Omega(i(\omega_n+\omega_\mu),\, i(\omega_{n+\nu+\mu}))} \frac{y^2}{\omega_\mu^2+y^2}\,\Lambda(i\omega_{n+\mu},\, i\omega_{n+\mu+\nu})\ , \tag{14}$$

where

$$\Omega(i\omega_1, i\omega_2) = (\tilde\omega_1^2 + \tilde\Delta_1^2)^{1/2} + (\tilde\omega_2^2 + \tilde\Delta_2^2)^{1/2} \tag{15}$$

and $P_2(z)$ is Legendre's polynominal. Here we made use of the same transformation as used in the calculation of the self-energy correction; we first replaced the three-dimensional integral $d^3p/(2\pi)^3$ by $N(0)\,d\xi_p\,d\Omega/4\pi$ where $\xi_p = p^2/2m - \mu$ and integrated over ξ_p, then we transformed the integral over Ω to that on the phonon energy $y = \omega_g$ by making use of the relation

$$\omega_q = Sp_0[2(1-\cos\theta)]^{1/2}\ .$$

$P_2(z)$ appears in Eq. (14), because the stress tensor in the limit $ql \ll 1$ has d-wave character. In the evaluation of the ultrasonic attenuation constant for low frequency [i.e., $\omega \ll \Delta(T)$, where ω is the sound wave energy], we need only the value of $\Lambda(i\omega_n, i\omega_{n+\nu})$ at $\Lambda(\omega+i\delta,\ \omega-i\delta)$. Within the first-order approximation $\Lambda(\omega+i\delta,\ \omega-i\delta)\ [\equiv\Lambda(\omega)]$ is evaluated then as

$$\Lambda(\omega) = \left[1 - \frac{\pi\lambda_0}{\omega_0^2}\int_0^\infty dy\,\frac{y^2 P_2(1-2y^2/\omega_0^2)}{|(\omega+y)/[(\omega+y)^2-\Delta^2]^{1/2}|\,a_1}\right.$$

$$\left.\times\left(\frac{2}{e^{y/T}-1} + \frac{2}{e^{y+\omega/T}-1}\right)\right]^{-1} \simeq \left(1 - \frac{a_2}{a_1}\right)^{-1} \tag{16}$$

and

$$a_2 \simeq \frac{2\pi\lambda_0}{\omega_0^2}\int_0^\infty dy\,y^2 P_2\left(1 - \frac{2y^2}{\omega_0^2}\right)\left(\frac{1}{e^{y/T}-1} + \frac{1}{e^{y+\omega/T}-1}\right). \tag{17}$$

For a metal with a single conduction band we will have

$$a_2 = a_1 + CT^5\ . \tag{18}$$

From this it follows that the mean free path relevant for the ultrasonic attenuation has a T^5 temperature dependence. However (see Sec. III A), in the ultrasonic attenuation in Nb, a T^3 dependence appears. We believe that this is because niobium has at least two distinct bands[15] with different electron masses. Then a_1 is described as the sum of two contributions, interband scattering and intra-

band scattering, while a_2 is due mostly to intraband scattering [the interband scattering contribution to a_2 has a small factor m_2/m_1, where m_2/m_1 is the ratio of the two effective masses of the respective bands (we assume that $m_2 \ll m_1$)].

C. Effective Mean Free Path

Making use of the above calculations, the effective mean free path of electrons, which appears in the calculation of the ultrasonic attenuation, is given by

$$l(\omega) = v_0\left\{2\,\text{Im}(\tilde\omega^2 - \tilde\Delta^2)^{1/2}[1 - \Lambda(\omega)]\right\}^{-1}$$

$$= \left(l_0^{-1} + \frac{|\omega|}{(\omega^2 - \Delta^2)^{1/2}}\,\theta(|\omega| - \Delta)BT^3\right)^{-1}\ , \tag{19}$$

where

$$BT^3 = v_0^{-1}(a_1 - a_2) \tag{20}$$

and v_0 is the Fermi velocity of the main band. On the other hand, the relevant mean free path in the normal state is obtained by simply letting $\Delta = 0$ in Eq. (19):

$$l_n = (l_0^{-1} + BT^3)^{-1}\ . \tag{21}$$

It has to be emphasized that the T^3 terms in Eqs. (19) and (21) result from the possible interband scattering of electrons due to the electron-phonon interaction in a two-band metal. In the case of a single-band metal we will have, instead of a T^3 term, a T^5 term.

D. Ultrasonic Attenuation Coefficient

Making use of the mean free path obtained in Eqs. (19) and (21), the ratio of the ultrasonic attenuation coefficient of both the longitudinal and the transverse sound waves with $gl \ll 1$ is given by[16]

$$\frac{\alpha_s}{\alpha_n} = \int_\Delta^\infty \frac{d\omega}{2T}\,l(\omega)\cosh^{-2}\left(\frac{\omega}{2T}\right)\Big/$$

$$\int_0^\infty \frac{d\omega}{2T}\,l_n(T)\cosh^{-2}\left(\frac{\omega}{2T}\right)\ . \tag{22}$$

At low temperatures where $l_0 BT^3 \ll 1$, Eq. (22) reduces to the BCS expression Eq. (1). Therefore, the gap determined at low temperatures making use of Eq. (1) should give the BCS gap $\Delta(0)$.

On the other hand, in the immediate vicinity of the transition temperature where $\Delta(T)/2T$ is small, Eq. (22) is expanded in powers of $\Delta(T)/2T$ and we have[17]

$$\frac{\alpha_s}{\alpha_n} = 1 - \frac{\Delta(T)}{2T}\,f(x)\ , \tag{23}$$

where

$$f(x) \equiv \lim_{\Delta \to 0} \left(\Delta \int_{\Delta}^{\infty} d\omega \; \frac{\omega}{(\omega^2 - \Delta^2)^{3/2}} \; \frac{x(1+x)}{[1 + x|\omega|/(\omega^2 - \Delta^2)^{1/2}]^2} \right)$$

$$= x(1+x) \int_{0}^{\infty} d\theta \; \frac{\cosh\theta}{(\sinh\theta + x\cosh\theta)^2} \tag{24}$$

$$= \begin{cases} \dfrac{1}{1-x}\left[1 - \dfrac{x^2}{(1-x^2)^{1/2}} \, \mathrm{arccosh}\left(\dfrac{1}{x}\right)\right] & \text{for } x < 1 \\[3mm] \dfrac{1}{x-1}\left\{\dfrac{x^2}{(x^2-1)^{1/2}}\left[\dfrac{\pi}{2} - \arcsin\left(\dfrac{1}{x}\right)\right] - 1\right\} & \text{for } x \geq 1 \end{cases} \tag{25}$$

and

$$x = l_0 B T_c^3 . \tag{26}$$

The x dependence of $f(x)$ is shown in Fig. 1. $f(x)$ increases monotonically as x increases. In particular, we have $f(0) = 1$, $f(1) = \frac{4}{3}$, and $f(\infty) = \frac{1}{2}\pi$. The BCS expression[1] corresponds exactly to the case $x = 0$, where the mean free path is determined by l_0 only.

Equation (23) predicts that $\Delta(0)_{ap}$, which is determined from data obtained near T_c, is larger than the true energy gap measured at low temperatures, and the ratio is given by

$$\frac{\Delta_{ap}(0)}{\Delta_{BCS}(0)} = f(x) . \tag{27}$$

In closing this section we will summarize the theoretical conclusions.

(i) In order to have a T^3 term in the electron mean free path for the attenuation coefficient, it is necessary to take account of the possible interband scattering due to phonons (i.e., two-band model).

(ii) Then the electronic mean free path in the normal state is given by

$$l_n^{-1} = l_0^{-1} + B T^3 , \tag{28}$$
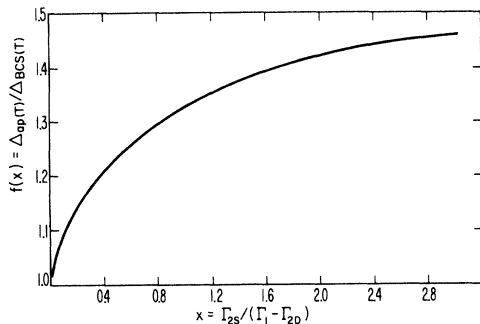
where B is related to the electron-phonon scattering by

$$B = v_0 \left(\frac{2\pi\lambda_0}{\omega_0^2} \, 7\zeta(3) T^3 \right)_{\text{interband}} . \tag{29}$$

(iii) The ratio of the two energy gaps measured in the vicinity of T_c and at low temperatures is given by Eq. (27). Hence, from the determination of this ratio we can determine the constant x in Eq. (26). Alternatively, we can estimate x in Eq. (26) by making use of the ultrasonic attenuation data in the normal state, and then we can test relation (27).

It has to be borne in mind that we neglect any other possible sources which could cause the ratio $\Delta_{ap}(0)/\Delta_{BCS}(0)$ to deviate from 1, such as the effect of anisotropy on the energy gap and also the effect of strong coupling since these effects appear to be of minor importance in the present problem, although they may affect our analysis slightly.

III. EXPERIMENTAL RESULTS

We have employed the pulse-echo technique on three samples of niobium[18] having different crystallographic orientation and purities (see Table I). Data were taken using a Matec attenuation comparator and attenuation recorder. The phonons were generated in quartz transducers having a 15-MHz fundamental. The transducers were wrung on the crystal with fresh (Fisher) Nonaq stopcock grease after driving out the accumulated water at 160 °C in the normal way. Normal-state data below the transition temperature were taken by driving the sample normal with the minimum required magnetic field.

The data were analyzed and are presented here with two purposes in mind. In Sec. III A the prediction $l^{-1} = l_0^{-1} + B T^3$ is tested; in Sec. III B the ratio $\Delta_{ap}(0)/\Delta_{BCS}(0) = f(x)$ is evaluated.

A. Mean Free Path

Here the data are compared with the model $l^{-1} = l_0^{-1} + B T^3$. In order to check the hypothesis that the mean free path is proportional to T^3, the normal-state data were compared with a theoretical model based on Pippard's[19] result

FIG. 1. Predicted ratio $f(x)$ for increasing purity (increasing x).

TABLE I. Summary of all relevant statistics and conclusions for the three samples investigated.

	Nb No. 2	Nb No. 3	Nb No. 8
$\rho_{300}/\rho_{4.2}$	>150	300	1000
Orientation	[111]	[100]	[110]
Length (cm)	1.27	2.54	1.11
Phonon	Trans.	Long.	Long.
Frequency (MHz)	135	225	45, 105
ql	0.36	0.40	0.6, 1.4
$\alpha_n - \alpha_s\mid_{t\to 0}$(Np/cm)	0.13	0.87	0.30, 1.28
T_c	9.21	9.24	9.39
l_0 (10^{-4} cm)	1.2 ± 0.2	1.6 ± 0.3	9.0 ± 0.1
B (1/°K³)	0.85 ± 0.15	1.0 ± 0.1	0.73 ± 0.05
$2\Delta(0)/kT_c$, $T \ll T_c$	3.70 ± 0.02	3.64 ± 0.02	4.04 ± 0.02
			3.84 ± 0.02
$2\Delta(0)/kT_c$, $T \simeq T_c$	4.24 ± 0.02	4.40 ± 0.02	6.12 ± 0.05
			5.68 ± 0.05
x_{normal}	0.08	0.13	0.55
$\Delta_{\text{ap}}(0)/\Delta_{\text{BCS}}(0)$	1.15 ± 0.02	1.21 ± 0.02	1.52 ± 0.02
			1.48 ± 0.02
$f(x_{\text{normal}})$	1.095	1.11	1.24
x_{sc}	0.23 ± 0.2	0.40 ± 0.06	6.8 ± 2

$$\frac{\alpha}{\alpha'} = \frac{6}{\pi}\left(\frac{1}{3}\frac{ql\tan^{-1}ql}{ql - \tan^{-1}ql} - \frac{1}{ql}\right) , \qquad (30)$$

where

$$\alpha' = \frac{\pi}{12}\frac{N_m v_0 \omega}{\rho_0 v_1^2} .$$

In this equation, we have imposed the condition $l^{-1} = l_0^{-1} + BT^3$. The zero-temperature mean free path l_0 is determined through comparison of (30) with data obtained for various frequencies at $T \simeq 1.3$ °K. The constant B is taken such that the agreement between experiment and theory extends as high in temperature as possible without compromising the fit for $T < T_c$. In all cases the theoretical fit is excellent for $T < T_c$ and begins to deteriorate at larger values of temperature.

Figure 2 shows normal and superconducting data for our intermediate purity sample, Nb No. 3. The solid line is found from Eq. (30). In this case, $l_0 = 1.6 \times 10^{-4}$ and $B = 1.0/$°K³. Clearly, the data and experiment are in good agreement. Data obtained in the superconducting state from the transition temperature 9.24 down to 1.2 °K are also shown in this graph.

Figure 3 shows normal-state data for Nb No. 8 at two frequencies, 45 and 105 MHz, where the fourth and first echoes were measured, respectively. Both theoretical lines are derived using Eq. (30). The same values for l_0 and B, along with the appropriate value of q for the two frequencies, are used to generate the two different curves. For this higher-purity sample, the fit of the curves to the experimental data is good for the 45-MHz data which have ql of 0.6, but deteriorates more quickly

for 105-MHz data. The higher-frequency data have $ql = 1.4$, and it is expected that as ql increases, the conclusions in Sec. II are no longer valid.

Previous work[20] had indicated for niobium a relationship $l^{-1} = l_0^{-1} + BT^3 + cT^5$ with the result $B/c \simeq 10^6$. The use of the T^5 "best-fit" approach
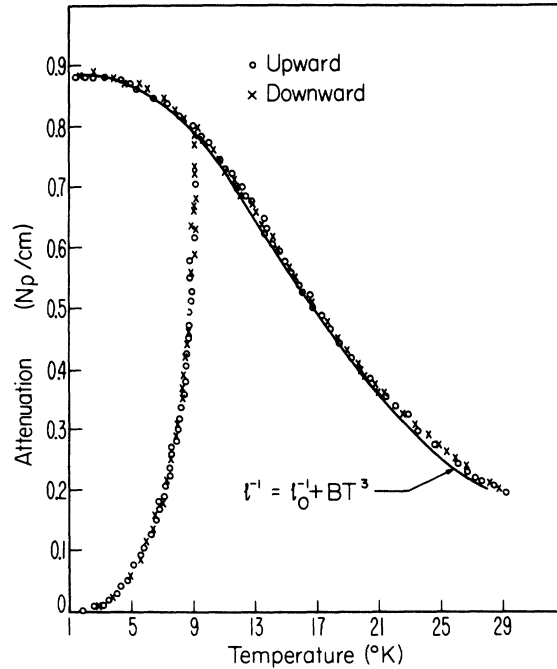

FIG. 2. Ultrasonic attenuation in the normal and superconducting states for Nb No. 3, at 255.5 MHz with a theoretical curve (solid line) for the T^3 case.
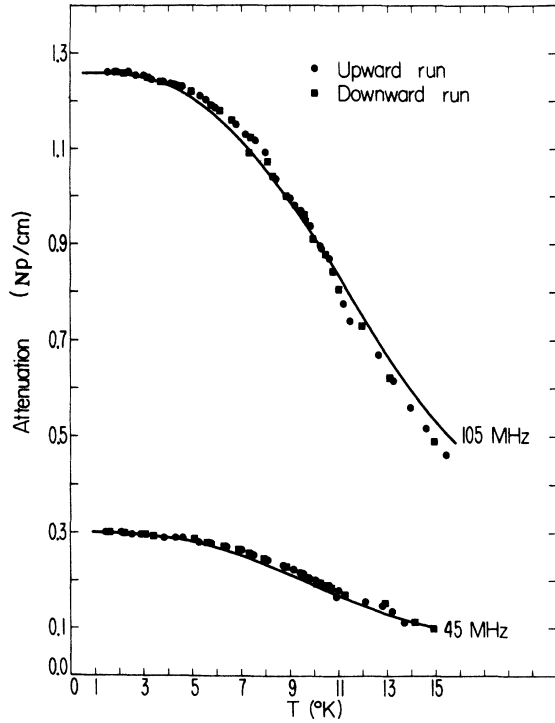
FIG. 3. Ultrasonic attenuation in the normal state in Nb No. 8 at 45 and 105 MHz. Here both theoretical (solid) lines are drawn using the same constants and the appropriate frequencies.

for these data yielded $B/c \simeq 10^3$ and reduced the value of B by nearly 50%. Therefore, in view of the information carried in B, the small apparent improvement in fit produced by considering a T^5 term was forfeited.

Some attention should be focused on the uncertainties of the results shown in Table I. The zero-temperature mean free path l_0 is measured by comparing data for different frequencies as described above. In most experimental arrangements a frequency change meant, in addition, a change of the comparison echo method. For example, the data for Nb No. 8 at 45 MHz were taken comparing the size of the first and fifth echo, while the 105-MHz data by that sample were taken comparing the first echo with a fixed standard. These techniques introduce an uncertainty of perhaps 3% when the data at the two frequencies are compared. This uncertainty leads to an uncertainty of 10% in the value of B as compared to the 2% uncertainty introduced by the scatter in data. This scatter is due to drift and noise in the apparatus.

If in the limiting case $ql \ll 1$, the phonons do average a large portion of the Fermi surface, a single value of B should exist such that $l^{-1} = l_0^{-1} + BT^3$ is a good fit to data in a temperature regime in ex-

cess of $0 < T < T_c$.[20] For our samples this is not entirely the case. The value of B which is most nearly compatible with all three samples, namely, $B = 0.85$, yields for sample No. 8 at $T = T_c$ a 7% deviation from the ultrasonic-attenuation data in the normal state.

The unsatisfactory fit to the normal data in sample No. 8 may be due to the fact that Eq. (30) is an exact result only for metals whose Fermi surface is spherical; there is evidence that for real metals Eq. (30) will require modification. The need for this modification is more apparent in the study of purer samples as our data seem to indicate. The modification of Eq. (30) will result in a different value for B.

B. Apparent Energy Gap

Here the ratio $\Delta_{ap}(0)/\Delta_{BCS}(0)$ is compared with the theoretical value of $f(x)$. Equation (1) can be written

$$\frac{T_R}{\Delta/kT_c} = [\ln(2\alpha_n/\alpha_s - 1)]^{-1} , \qquad (31)$$

where $T_R = T/T_c$. When $T_R < 0.6$ the energy gap changes very slowly so that a plot of T_R vs $[\ln(2\alpha_n/\alpha_s - 1)]^{-1}$ should tend to a straight line with slope $= [\Delta_{BCS}(0)/kT_c]^{-1}$ in this regime.

Figure 4 shows such a plot for Nb No. 8 at 105 MHz. For this sample, $2\Delta_{BCS}(0)/kT_c = 3.84$. This analysis is also used to determine the absolute value of the electron-phonon interaction contribution to the total ultrasonic attenuation. Other attenuations and losses[21] are assumed to be temperature independent, and therefore a constant amount is subtracted from the total attenuation to take into account these losses. This amount is chosen such as to yield a linear extrapolation of the straight line to the origin, as shown in Fig. 4.
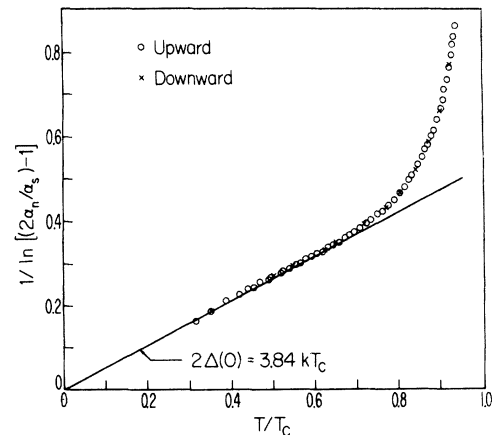

FIG. 4. Low-temperature data analysis for Nb No. 8 at at 105 MHz. The limiting slope is $1/\Delta_{BCS}(0)$.
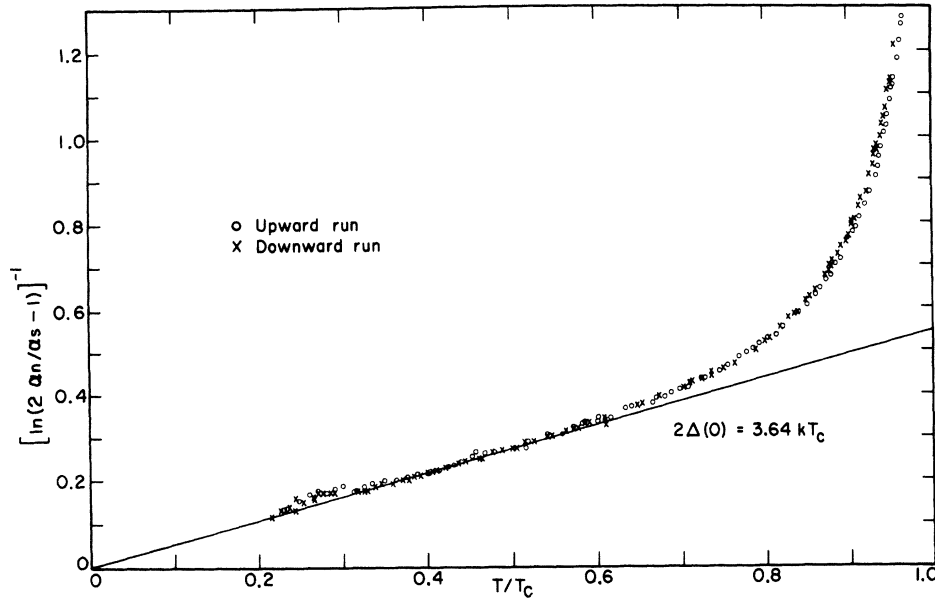
FIG. 5. Low-temperature data analysis for Nb No. 2 at 135 MHz. The slope as $T \to 0$ is the inverse of the energy-gap parameter.

Figure 5 shows the same analysis of data from Nb No. 3 at 225.5 MHz. The result is $2\Delta_{BCS}(0) = 3.64kT_c$. The scatter present at lower temperatures is due to the small size of the ultrasonic attenuation in the superconducting state compared to noise and drift.

In the region just below the transition temperature $\Delta_{ap}(0)$ may be conveniently measured by comparing the experimental ratio of α_s/α_n with the ratio predicted by (1). The theoretical value of α_s/α_n is found by letting

$$\Delta(T) = [\Delta(T)/3.5kT_c]_{BCS} \Delta_{ap}(0)$$

and varying $\Delta_{ap}(0)$ until a good fit to the data is achieved. The experimental α_s/α_n values are found by dividing α_s data by the corresponding α_n obtained from the smoothed data as discussed in Sec. III A.

Figure 6 shows the data obtained from Mb No. 3 at 225.5 MHz compared with two theoretical lines; one line is the BCS weak-coupling value $2\Delta(0) = 3.5kT_c$ the other line with $2\Delta(0) = 4.24kT_c$ is a "best fit" for the region $T \simeq T_c$.

Figure 7 shows a somewhat similar analysis for Nb No. 8 at 105 MHz. Here the data are compared to the "best fit" given by $2\Delta_{ap}(0) = 5.08kT_c$ and with the low-temperature value $2\Delta_{BCS}(0) = 3.84kT_c$ called the BCS energy gap. In this graph, departure from BCS-type behavior is similar to, but much more pronounced than, that in Fig. 6. Furthermore, the points for $T_R < 0.5$ show an unmistakable preference for the curve obtained using the smaller gap.

The ratios $\Delta_{ap}(0)/\Delta_{BCS}(0)$ are readily evaluated for the three samples yielding 1.15, 1.21, and

1.50 for Nb No. 2, Nb No. 3, and Nb No. 8, respectively. On the other hand, we can calculate these ratios making use of x determined from the mean free path in the normal state. We find these ratios to be 1.095, 1.11, and 1.24, respectively, which would account for about one-half of the deviation from unity of this ratio.

IV. DISCUSSION AND CONCLUSION

In our previous discussion, we were concerned with the electronic mean free path, which yields the value for x. Making use of the x determined in this manner, we can account for roughly one-half of the deviation from unity of the ratio $\Delta_{ap}(0)/\Delta_{BCS}(0)$ observed. We will now turn the procedure around; taking the observed ratio $\Delta_{ap}(0)/\Delta_{BCS}(0)$ in Eq. (27), we obtain $x = 0.23 \pm 0.2$, 0.40 ± 0.06, and 6.8 ± 2 for Nb No. 2, Nb No. 3, and Nb No. 8, respectively. These values are roughly a factor of 3 larger than the corresponding x's determined from the electronic mean free path in the normal state. At present we are unable to explain these discrepancies. However, the anisotropy in the energy gap would most likely contribute to this discrepancy, although we cannot give any reasonable estimate of this effect.

Going back to the electron-phonon scattering part of the electronic mean free path, we find for all our samples $B \cong 0.85/°K^3$ cm, which indicates that the electron-phonon scattering contribution is not influenced by the impurity scattering. This is consistent with the idea that the contribution to the inverse lifetime due to impurity scattering is simply additive for low-impurity concentration. We can also estimate B purely theoretically by
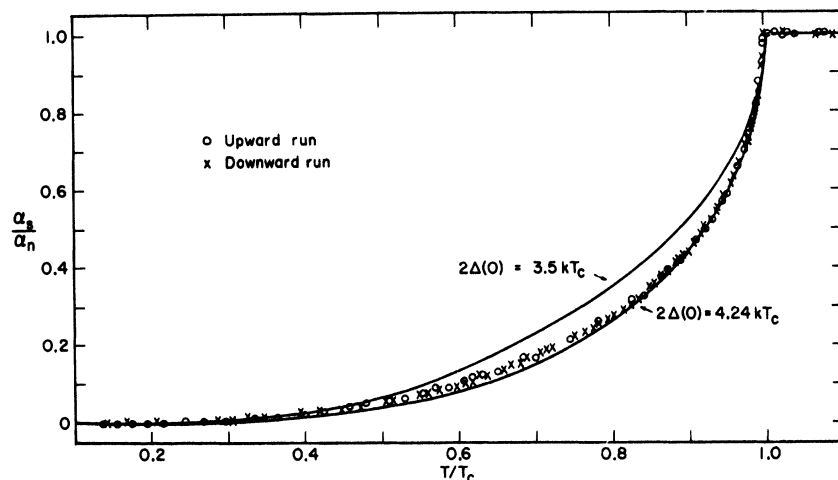
FIG. 6. Attenuation ratio α_s/α_n for Nb No. 3 at 255.5 MHz compared with the theoretical (solid) line drawn using $2\Delta(0) = 4.24 k T_c$. In taking the ratio a smoothed average is used for α_n.

making use of Eq. (29). Of course, we do not know the parameters involved for interband scattering. For intraband scattering we have $B \cong 1.2/°K^3$ cm, where we made use of the following values: $\lambda_0 = 0.82$, $\omega_0 = 277$ °K (here instead of ω_0 we made use of the Debye frequency Θ_0, which is of the same order of magnitude),[22] and $v_0 = 3 \times 10^7$ cm/sec. We may say that the B determined above is consistent with this theoretical estimate. A few comments are in order about the effect of the anisotropy of the energy gap. Table I shows that there is a slight variation in $\Delta_{BCS}(0)$ for the three niobium samples. It is reasonable to expect that these values should be equal to each other if the sound propagation were along the same crystallographic axis for the three samples, even though they have different impurity contents. In fact, this is a principal conclusion of the present work. However, the orientations are different. One could ascribe these differences to gap anisotropy, a fact which has been observed using the ultrasonic waves with $ql > 1$.[7] In this high-frequency case, gap anisotropy should be observed, since the interacting electrons have a velocity component in the direction of the sound propagation equal to the sound velocity. Thus, the sound wave is sampling a perpendicular cross section of the Fermi surface. In our case, however, $ql < 1$ and the weighting becomes much broader. In the case of longitudinal waves the interaction samples the gap preferentially in some directions, since the attenuation coefficient is proportional to $[P_2(z)]^2 = [\frac{1}{2}(3z^2 - 1)]^2$, where $z = \cos\theta$ and θ is the aximuthal angle between the propagation direction and the Fermi wave vector. Thus, when sound is propagated along different orientations, different portions of the Fermi surface are sampled.[23] Therefore, gap anisotropy may account for the three samples. In addition to simple anisot-

ropy, sample No. 8 shows a definite frequency dependence in energy gap. This is taken to be the same ql dependence as described above and previously reported.[7]

In the above theoretical calculation we have assumed implicitly a weak electron-phonon interaction; we calculate the effects of electron-phonon interaction by essentially making use of first-order perturbation.

Therefore, it may be possible to improve the agreement slightly, if we take account of the strong-coupling effect between electrons and phonons in niobium.

In summary, we find that the anomalously large energy gap measured near $T = T_c$ for pure niobium using ultrasonic attenuation with $ql < 1$ can be understood partly in terms of a shortening of the mean free path of electrons with small excitation energy
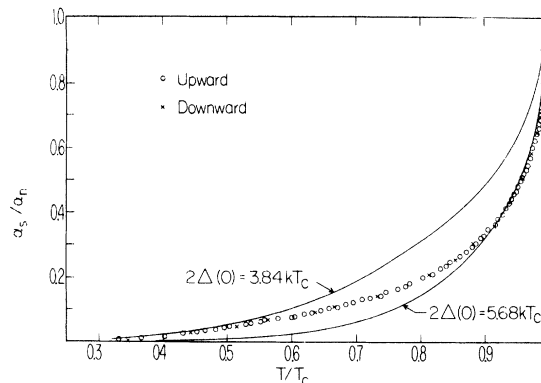

FIG. 7. Attenuation ratio α_s/α_n for Nb No. 8 at 105 MHz compared with the theory (solid line) for two values of $2\Delta(0)$, the low-temperature value (Fig. 4) and the best-fitted value.

in the superconducting state. This shortening is related to the fact that the quasiparticle velocity vanishes at the gap edge in the superconducting state. A detailed analysis of experimental data indicates that this shortening effect explains about one-half of the deviation of the ratio $\Delta_{so}(0)/\Delta_{BCS}(0)$ from unity. It is quite likely that the remaining half can be explained as well in terms of the electron-phonon scattering, although we cannot discard other possibilities[24] such as the anisotropy of the energy gap for the moment. Further experiments on purer niobium samples should clarify these points.

†Research sponsored by the Air Force Office of Scientific Research under AFOSR Grant No. 70-1847.

*Present address: Department of Physics, University of Southern California, Los Angeles, Calif.

‡Present address: Department of Physics, University of Wisconsin—Milwaukee, Milwaukee, Wisc.

[1]J. Bardeen, L. N. Cooper, and J. R. Schrieffer, Phys. Rev. 108, 1175 (1957).

[2]T. Tsuneto, Phys. Rev. 121, 402 (1961).

[3]L. T. Claiborne and R. W. Morse, Phys. Rev. 136, A893 (1964).

[4]J. R. Leibowitz, Phys. Rev. 133, A84 (1964).

[5]M. Levy, Phys. Rev. 131, 1497 (1963).

[6]P. Wyder, Rev. Mod. Phys. 36, 116 (1964); Physik Kondensierten Materie 3, 292 (1965).

[7]E. R. Dobbs and J. M. Perz, Rev. Mod. Phys. 36, 257 (1964).

[8]M. Levy, R. Kagiwada, and I. Rudnick, Phys. Rev. 132, 2039 (1963).

[9]T. Suzuki and N. Tsuda, J. Phys. Chem. Solids 28, 2487 (1967).

[10]E. M. Forgan and C. E. Gough, Phys. Letters A26, 602 (1968).

[11]F. Carsey, S. Jacques, R. Kagiwada, and M. Levy (unpublished).

[12]G. M. Eliashberg, Zh. Eksperim. i Teor. Fiz. 39, 1437 (1960) [Sov. Phys. JETP 12, 1000 (1961)].

[13]A. A. Abrikosov, L. P. Gor'kov, and I. E. Dyaloshinski, *Methods of Quantum Field Theory in Statistical Physics* (Prentice-Hall, Englewood Cliffs, N. J., 1963).

[14]L. P. Kadanoff and P. C. Martin, Phys. Rev. 124, 670 (1961).

[15]L. F. Mattheiss, Phys. Rev. B 1, 373 (1970).

[16]K. Maki, Physik Kondensierten Materie 8, 305 (1969).

[17]K. Maki, Progr. Theoret. Phys. (Kyoto) 41, 586 (1969).

[18]Electron-phonon interaction in the mixed state of Nb No. 2 and Nb No. 3 was reported in R. Kagiwada, M. Levy, I. Rudnick, H. Kagiwada, and K. Maki, Phys. Rev. Letters 18, 14 (1967).

[19]A. B. Pippard, Phil. Mag. 46, 1104 (1955).

[20]G. W. Webb, Phys. Rev. 181, 1127 (1969).

[21]R. Truell, C. Elbaum, and B. Chick, *Ultrasonic Methods in Solid State Physics* (Academic, New York, 1969).

[22]W. L. McMillan, Phys. Rev. 167, 331 (1968).

[23]The differences in values of the $\Delta_{BCS}(0)$ for different orientations are more difficult to analyze than the differences found through tunneling, since tunneling experiments involve averaging over better-defined "windows" on the Fermi surface, R. M. Rose (private communication).

[24]J. W. Hafstrom and M. L. A. MacVicar, Phys. Rev. B 1, 375 (1970), introduce the possibility of a nonzero gap for s electrons near T_c for the d electrons. The influence of this gap on the ultrasonic attenuation coefficient has been estimated for the mixed state [I-Ming Tang, Phys. Rev. B 2, 2581 (1970)] but not for this case.